How periodic are terahertz quantum cascade lasers?

T Kubis and P Vogl

Walter Schottky Institute, Technische Universität München, Am Coulombwall 3, 85748 Garching, Germany

E-mail: tillmann.kubis@wsi.tum.de

Abstract. We apply a novel non-equilibrium Green's function method for open quantum devices to analyze quantum cascade lasers. We find the carrier distribution in typical resonant phonon THz-QCLs to develop a periodicity that differs from the geometric periodicity of the QCL. We propose a design improvement that thermalizes electrons at threshold bias and thereby pins the electron density to the QCL periodicity.

1. Introduction

Quantum cascade lasers (QCLs) have been studied experimentally [1] and theoretically. The theoretical approaches used most commonly are the density matrix method [2, 3], the Boltzmann equation [4, 5], and the non-equilibrium Green's function method (NEGF) [6, 7]. All of these theoretical studies share the common approximation of invoking field periodic boundary conditions.

We have developed a self consistent non-equilibrium Green's function method (NEGF) for stationary charge transport in open THz-QCL devices that are attached to dissipative leads [8]. Importantly, our method differs from previous models by not imposing field-periodic boundary conditions. Instead, the electrons can enter and leave the device via travelling eigenstates of the semi-infinite leads. This allows us to capture non-periodic phenomena as well as investigate spatially extended, energetically high lying states.

The primary goal of this paper is to illustrate the formation of electron distributions in resonant phonon THz-QCLs that are commensurable or incommensurable with the QCL device periods. We show the impact of such distributions on the device current density and the optical gain. Finally, we propose a design modification that pins the electrons to the QCL periodicity.

2. Method

We use the non-equilibrium Green's function method (NEGF) to calculate stationary electronic transport and optical gain up to the threshold current in a single conduction band with an effective mass $m^*(z)$. We assume the QCLs to be homogeneous in the lateral x,y directions and to be in contact with two equilibrium reservoirs at $z=0$ and $z=L$, respectively. Thereby, we consider charge transport as a scattering problem from source to drain with the QCL structure being the active device. The source and drain leads are assumed to consist of QCL periods by themselves, albeit with zero electric field and with the carriers obeying equilibrium Fermi statistics. In this way, we mimic adjacent QCL periods. The electrons enter the device in propagating eigenstates of the respective infinitely extended lead Hamiltonians [8]. We take into account inelastic acoustic and polar-optical phonon scattering, scattering by charged impurities, interface roughness, and by electron-electron interaction in the

Hartree approximation. The scattering self-energies are determined in the self-consistent Born approximation including their full nonlocal momentum and energy dependence. The electrostatic potential Φ is determined self-consistently with the Green's functions by solving the Poisson equation under the condition of global charge neutrality and unambiguous bias value. We calculate the optical absorption coefficient in linear optical response, taking into account the calculated laser states and non-equilibrium state occupations, but ignoring vertex corrections to the self energies. Details of the method are given in [8].

3. Results and Discussion

We consider electron transport in the resonant phonon THz-QCL structure of [9] which consists of 271 identical periods of GaAs and $Al_{0.15}Ga_{0.85}As$ layers of the widths (30) 92 (55) 80 (27) 66 (41) 155 Å. The values in parentheses indicate the $Al_{0.15}Ga_{0.85}As$ barriers and the underlined well is the only doped region with a doping density of 1.9×10^{10} cm^{-2}. We calculate charge transport in terms of two models. In one model, we treat a single device period as active device, whereas the other model includes explicitly two device periods. In both models, the remaining periods are included in the leads as described above. In figure 1, we depict the calculated (black) and experimental (gray dots) I-V characteristics of this QCL. Both models agree with one another and reproduce the experimental data of the QCL up to the threshold bias. In the remainder of this section, we focus on the two-periods model.

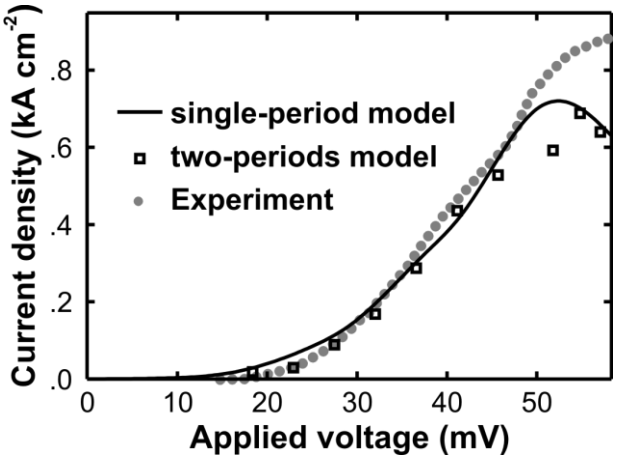

Figure 1. Calculated current density as a function of applied bias voltage per period of the QCL of [9] at 40K and a sheet doping density of 1.9×10^{10} cm^{-2} and comparison to experiment [9]. The results of the single-period model (line) and two-periods model (squares) agree well with experiment (dots).

We will show now that for low carrier concentration, the electronic states follow the QCL periodicity, in sharp contrast to the carrier density that deviates from periodicity. In figure 2 (a), we show the contour plot of the spectral function at vanishing in-plane momentum in two adjacent periods of the QCL for a bias of 52 mV/period. The maxima of this spectral function correspond to resonant electronic states. The states associated with the first and second QCL period are labeled by numbers and primed numbers, respectively. In both periods, the injector states (5 and 5') are seen to be aligned with the upper laser states (4 and 4'), whereas the lower laser states (3 and 3') are aligned with the collector well states (2 and 2'). We point out that the energy difference between the lower laser levels (3 and 3') and the lowest collector states (1 and 1') match the energy of an LO-phonon *in both periods*. Nevertheless, we find the carrier distribution to deviate from the geometric QCL periodicity. This can be seen most clearly by a contour graph of the local energy resolved current density *j(z,E)* (as defined, e.g., in [6]). Figure 2 (b) shows this quantity for the same bias as in part (a). The function *j(z,E)* shows spatially constant (i.e. horizontal) stripes in regions where the electrons propagate without dissipating energy. Disruptions of these horizontal stripes mark positions where LO-phonons get emitted. The figure shows that the number of emitted LO phonons is no longer equal for adjacent QCL periods. When the electrons have passed the first period and traversed a potential drop of 52 meV, they have emitted only one LO-phonon of energy 36 meV. The elastic and inelastic scattering mechanisms are not able to dissipate the remaining 16 meV within this QCL period. This is a

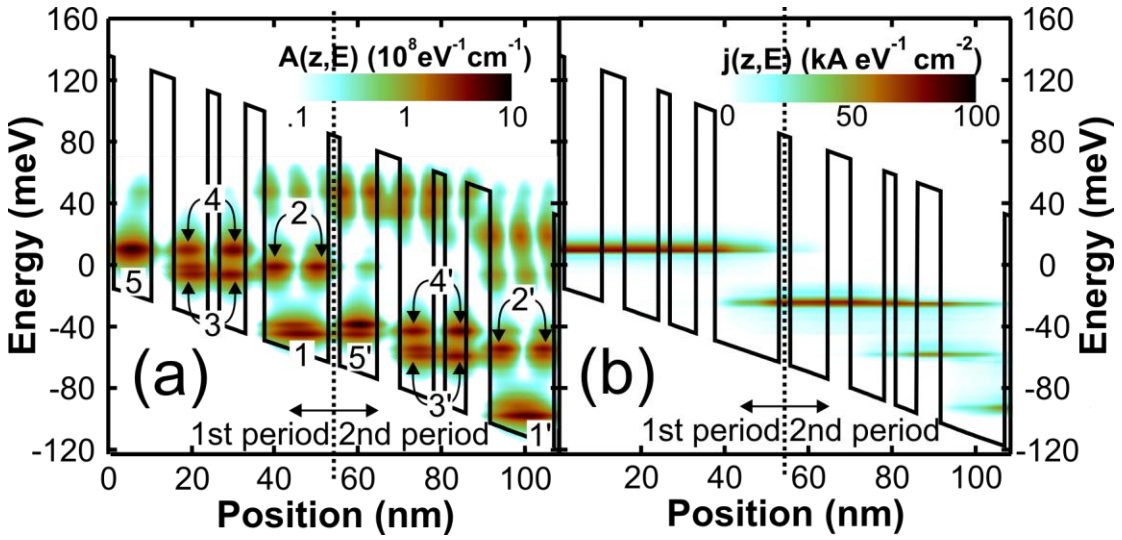

Figure 2. (a) Calculated conduction band profile (line) and contour plot of the energy and spatially resolved spectral function *A(z,E)* at vanishing in-plane momentum in two adjacent periods of the QCL at a bias voltage of 52 mV per period in the relevant energy range between -121 meV and 78 meV. The zero in energy marks the chemical potential of the source. The dotted line marks the boundary between first and second period. (b) Calculated spatially and energy resolved current density *j(z,E)* of the QCL in (a).

consequence of the good state alignment that supports efficient coherent multi-barrier tunneling [8]. Consequently, the electrons enter the second period with an in-plane kinetic energy of 16 meV. This can be seen in figure 2 (b); the energy of the leftmost current stripe coincides with states 5 and 4, whereas the following current stripe lies above the corresponding states 5' and 4'. Thus, these propagating electrons are now able to emit an LO-phonon, ending up in and occupying the lower laser level 3'. This occupancy leads to the build-up of the current stripe near *z=80* nm in Figure 2 (b) that is absent in the first period. The electrons can now tunnel resonantly from 3' into state 2' and scatter into the lowest collector state 1' by the emission of an additional LO-phonon. Thus, the electrons have emitted a total of 3 LO phonons (*3×36=108* meV) across 2 QCL periods (voltage drop of *2×52=104* meV) and are finally fully thermalized. The remaining small energy discrepancy can be gained from absorbing or emitting acoustic phonons. This process is repeated in the subsequent QCL periods such that we obtain a commensurable charge distribution with period two. Since the detailed energy balance depends on the applied bias voltage, the carrier density and current distribution may even become incommensurable with the geometric periods.

A consequence of this incomplete carrier thermalization is a significant reduction in the occupation inversion and the optical gain in every other period. Concretely, we find a drop of approximately 65% in the second period at the voltage shown in figure 2. We would like to point out that the periodic nature of the spectral function in figure 2 (a) is intimately related to the small carrier density that does not distort the conduction band profile in spite of the different charge density in the second QCL period. This explains the good agreement between the two models (one-period and two-periods) we have obtained in figure 1.

In order to estimate whether the inelastic electron-electron (e-e) scattering can relax the electrons and restore the periodicity of the carrier distribution to a single QCL period, we have calculated the Green's functions including the e-e scattering in the static GW_0 approximation. However, we find this type of e-e interaction to be unable to thermalize the non-equilibrium subband distribution sufficiently strongly [8].

4. QCL design for fully thermalized structure

We have seen the heated carrier distribution in the second period of the QCL in figure 2 to allow nonradiative transitions from the upper into the lower laser level. In order to pin the electron distribution to the QCL periodicity and thereby to prevent these nonradiative transitions, we propose a new QCL structure. We augment each QCL period from [9] by two additional layers, a 3 nm $Al_{.15}Ga_{.85}As$ barrier, followed by a 17.1 nm wide GaAs quantum well namely. This leads to a threshold bias of ~72 mV per period which results in a potential drop that is commensurable with the energy of two LO-phonons. The purpose of these additional layers is to allow the electrons to dissipate the 16 meV discussed above within the same QCL period rather than causing a nonperiodic density distribution. Figure 3 shows a contour plot of the energy and spatially resolved current density *j(z,E)*. Also shown in this figure are contour lines of the spectral function at vanishing in-plane momentum.

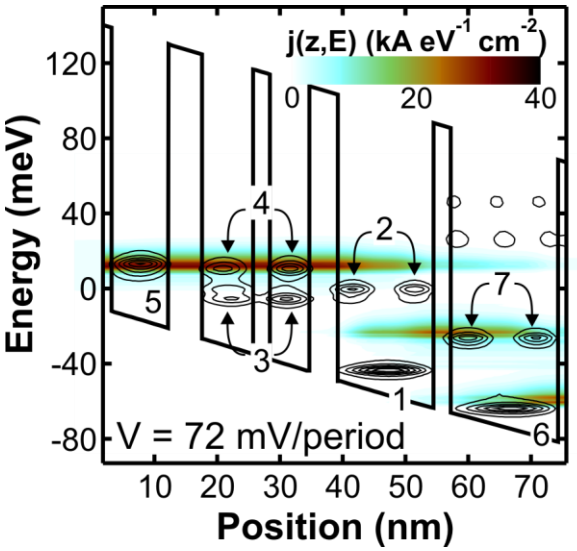

Figure 3. Calculated conduction band profile (thick line) and contour plot of the energy and spatially resolved current density *j(z,E)* in a single period of the proposed new QCL design described in the main text. The thin lines depict contour lines of the spectral function *A(z,E)* at vanishing in-plane momentum. The zero in energy marks the chemical potential of the source.

Most electrons that arrive in state 1 have a surplus of 16 meV of kinetic energy in the in-plane motion. Therefore, their total energy suffices to scatter into state 6 by the resonant emission of a second LO-phonon. This can be seen in figure 3 for positions *z=70* nm. Here, the dominant maximum of *j(z,E)* coincides with the state 6. Thus, the main portion of the carrier distribution at the end of the period is reset to its original value. In this way, the electrons are almost completely thermalized and nonradiative transitions between the laser states of this and the following QCL period are suppressed.

Acknowledgments

The authors acknowledge financial support from the Deutsche Forschungsgemeinschaft (SFB 631), the Österreichische Fonds zur Förderung der Wissenschaft (SFB IRON) and the Nano Initiative Munich.

References

[1] Belkin M A, Fan J A, Hormoz S, Capasso F, Khanna S P, Lachab M, Davies A G and Linfield E H 2008 Opt. Express **16** 3242
[2] Iotti R C and Rossi F 2001 *Appl. Phys. Lett.* **78** 2902
[3] Willenberg H, Döhler G H and Faist J 2003 *Phys. Rev.* B **67** 085315
[4] Jirauschek C and Lugli P 2008 *phys. stat. sol.* (c) **5** 221
[5] Gao X, Botez D and Knezevic I 2007 *J. Appl. Phys.* **101** 063101
[6] Wacker A 2008 *phys. stat. sol.* (b) **5** 215
[7] Zheng X, Chen W, Stroscio M and Register L F 2006 *Phys. Rev.* B **73** 245304
[8] Kubis T, Yeh C, Vogl P, Benz A, Fasching G and Deutsch C 2009 *Phys. Rev.* B **79** 195323
[9] Andrews A M, Benz A, Deutsch C, Fasching G, Unterrainer K, Klang P, Schrenk W and Strasser G 2008 *Mater. Sci. Eng.* B **147** 152